Synthesis of Template-Free Iron Oxyhydroxide Nanorods for Sunlight-Driven Photo-Fenton Catalysis

Arnab Samanta, Samir Kumar Pal,* and Subhra Jana*

Cite This: *ACS Omega* 2021, 6, 27905−27912

Read Online

ACCESS | Metrics & More | Article Recommendations | Supporting Information

ABSTRACT: Designing a photocatalyst with high efficiency using semiconductor materials emerges as a promising approach for the treatment of wastewater. At the same time, it is very essential to develop nondestructive, green, and sustainable techniques for the degradation of refractory pollutants. Here, we have demonstrated a facile route to prepare iron oxyhydroxide nanorods (β-FeOOH) without employment of any templating agent via a light-driven solution chemistry pathway and explored the as-prepared nanorods as the photo-Fenton catalyst under solar light irradiation. The photocatalytic experiments were performed toward the degradation of the aqueous solution of two different pollutants, namely, methylene blue and rhodamine B dyes. We have illustrated the effect of pH of the solution together with the concentration of H_2O_2 during the degradation process and optimized the solution pH as well as the H_2O_2 concentration. The superb photocatalytic efficiency of β-FeOOH is attributed to the generation of reactive oxygen species in the presence of solar light, and these photo-produced reactive oxygen species assist the degradation process. The excellent photocatalytic efficacy and sustainability of β-FeOOH nanorods along with their effortless synthesis approach point to a cost-effective and environmentally benign pathway in fabricating a highly active photocatalyst for the degradation of organic dyes.
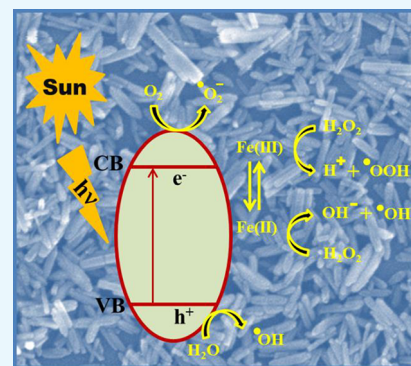
■ INTRODUCTION

In the 21st Century, environmental pollution has become a great concern to living systems on earth due to its adverse consequences. Among the various types of environmental pollutions, water pollution, which upsurges with the civilization of the society, not only is the biggest threat to aquatic lives but also has serious effects onto human health.[1−5] Such upsurge in water pollution is majorly due to the urban discharges together with industrial effluents, mainly organic dyes immensely utilized in food processing and textile industries.[6] Organic dyes owing to have a very complex structure are very harmful due to their toxicity and non-biodegradability.[7,8] Apart from the hazardous effects, they can also hamper the photosynthesis of aquatic plants. Therefore, it is necessary to degrade organic dyes to minimize their dreadful impact on aqueous environments. Many approaches have been reported to treat dyes in wastewater, including sedimentation,[9] flocculation and coagulation,[10] biodegradation,[11] membrane separation,[12,13] advanced oxidation process,[14,15] and adsorption methods.[16,17] Among all the approaches, the advanced oxidation method functions as a robust and very effective way to degrade organic dyes. In wastewater treatment, different advanced oxidation processes, such as photocatalysis,[18,19] electrochemical catalysis,[20] and the Fenton/photo-Fenton process,[21,22] have gained considerable attention from researchers. Fenton and photo-Fenton processes are unanimously used to oxidize organic pollutants by generating the transient species (·OH).[23] In the Fenton reaction, the ·OH radical produced from the decomposition of

H_2O_2 played a vital role during the treatment of refractory pollutants.[24,25] Alternatively, iron was cycling between Fe^{2+} and Fe^{3+} under irradiation of light in the case of photo-Fenton reaction and H_2O_2 was more effortlessly transformed to ·OH than that of Fenton reaction.[26,27] Therefore, to overcome the shortcoming of slow dynamics of the conventional Fenton process, photo-Fenton reaction is considered to be a smart way for the degradation of different organic dyes.

To date, there are many catalysts reported for heterogeneous photo-Fenton reactions; however, metal oxides are one of the most explored classes of photocatalytic materials from both the fundamental and technological point of view. Among the various photo-Fenton catalysts, iron-based materials, such as oxides,[28,29] sulfides,[30] carbides,[31] and composite materials,[26,32] demonstrate good photocatalytic activity. Iron oxides are non-hazardous, eco-friendly, and earth-abundant materials and can be prepared in the laboratory easily.[33,34] Thus, the development of iron oxide materials for photocatalysis is very simple and cost-effective. Earlier studies illustrated that iron oxides are very promising catalysts for heterogeneous Fenton-like

processes. The β-phase of iron oxyhydroxides (FeOOH), commonly known as akaganeite, has withdrawn enormous interests to researchers because of their biocompatibility along with abundances in nature. Additionally, they can efficiently harvest visible light in the solar spectrum due to their semiconducting property. However, the synthesis of such nanomaterials having high photocatalytic activity and stability is very challenging. Although several reports demonstrated the synthesis of β-FeOOH via various routes,[35,36] however, fabrication of β-FeOOH via a simple low-temperature light-assisted process might be an attractive pathway because of its simplicity and effectiveness.

Herein, we have reported a facile route to synthesize iron oxyhydroxide (β-FeOOH) nanorods without employing any templating agent via a light-driven hydrolysis route. After characterization of the synthesized nanorods by different physical techniques, we have explored them as a photo-Fenton catalyst and investigated their photocatalytic activity in the presence of H_2O_2 under sunlight. To understand the photocatalytic performance of β-FeOOH nanorods, we have chosen methylene blue (MB) and rhodamine B (RhB) as model refractory pollutants. We have also altered the reaction parameters including pH of the solution and concentration of H_2O_2 to realize the effect onto their photocatalytic activity. Additionally, excellent photocatalytic efficacy along with structural durability and stability has been discussed for β-FeOOH nanorods.

■ EXPERIMENTAL SECTION

Materials. All chemicals were used as received. Iron(III) chloride ($FeCl_3$) and *tert*-butanol (*t*-BuOH) were procured from Sigma-Aldrich. Urea, hydrogen peroxide (H_2O_2), and sulfuric acid were purchased from Merck. Methylene blue (MB), rhodamine B (RhB), and sodium hydroxide (NaOH) were obtained from Sisco Research Laboratory (SRL), India.

Preparation of Iron Oxyhydroxide Nanorods. Iron oxyhydroxide nanorods (FeOOH NRs) were prepared based on a simple and facile light-assisted hydrothermal technique[37] in the absence of any templating molecule. First, 1.0 mmol of iron(III) chloride ($FeCl_3$) and 2.5 mmol of urea were dissolved in 10 mL of Millipore water in a beaker. Then, the whole solution mixture was transferred to a glass vial and the vial was closed tightly. Afterward, the vial was kept for 24 h under visible light and the reaction temperature of the solution was maintained to 90 °C. Once the reaction was over, the vial was allowed to reach room temperature and the product was collected through centrifugation. The obtained product was washed properly with plenty of Millipore water to remove any unreacted urea or $FeCl_3$ if any and then dried in air. After proper air drying, the as-synthesized material was characterized by different techniques and explored as the photocatalyst for photo-Fenton reaction, as shown in Scheme 1.

Photo-Fenton Reaction. We have examined the photocatalytic activity of β-FeOOH nanorods by measuring the absorbance of the irradiated dye solution during the degradation of the aqueous solution of two different dyes under sunlight. All the reactions were performed in a cylindrical reactor vessel (50 mL), which was made of a borosilicate glass with a cooling water jacket. During the photocatalysis, we have placed the reactor in solar radiation under stirring conditions. The temperature for degradation was upheld to 25 °C throughout the experiment via circulating cold water. The photocatalytic degradation of the aqueous solution

Scheme 1. Schematic Representation of the Synthesis of β-FeOOH Nanorods Followed by the Exploration as a Photocatalyst for Photo-Fenton Reaction
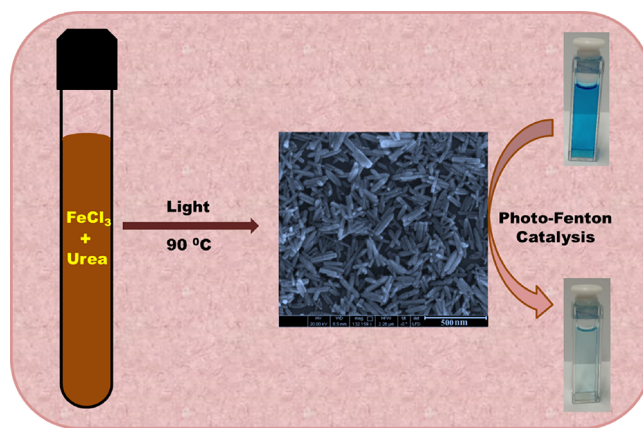
of methylene blue (MB) and rhodamine B (RhB) was checked as a function of time by measuring the absorbance of the irradiated solution with the help of a UV–vis spectrophotometer. Before exposing the dye to solar light irradiation, the FeOOH NRs having a concentration of 0.25 g L^{-1} were added to the aqueous solution of the dye (20 mL, 10 mg L^{-1}, and pH 3). The reaction mixture was then shaken well and kept in the dark for 2 h to attain an adsorption/desorption equilibrium. After the equilibrium, the initial concentration of the dye (C_0) was measured and then 50 mM H_2O_2 was added into this reaction solution immediately and subsequently exposed to solar light irradiation. To calculate the residual dye concentration, 3.0 mL of the dye solution was collected from the glass reactor at a specific time duration and the solution was used for absorbance measurement. Before recording the spectrum, the photocatalyst was separated from the reaction solution via centrifugation each time. Once the absorbance spectrum of the dye solution was recorded, it was then transferred back into the reactor. Afterward, the absorption spectra of solar light exposed MB were quantitatively evaluated at 664 nm with a definite time interval during the degradation process. Likewise, the absorption spectrum for RhB was considered at 554 nm for its degradation study. To check the photocatalytic activity at different pH, the pH of the dye solution was adjusted by using H_2SO_4 and NaOH solution. The percentage of degradation of dyes was determined as the following: % of degradation = $[(C_0 - C_t)/C_0] \times 100$, where C_0 is the initial dye concentration and C_t is the concentration of the dye after solar light irradiation at a time t.

■ RESULTS AND DISCUSSION

Iron oxyhydroxides (FeOOH) are achieved based on a simple light-assisted hydrothermal technique without the presence of any templating molecule, where urea functions as a hydrolyzing agent. The size and shape of the as-prepared FeOOH were visualized by field emission scanning electron microscopy (FESEM) and transmission electron microscopy (TEM) analysis. Figure 1A–C and Figure 1D,E display FESEM and TEM images of FeOOH NRs, respectively, which demonstrates the formation of FeOOH nanorods under the present synthetic conditions, having a length of ∼250 nm and diameter of ∼40 nm. The TEM micrograph of a single FeOOH nanorod is presented in Figure 1F. HRTEM images of this single FeOOH NR at diverse magnifications have been presented in
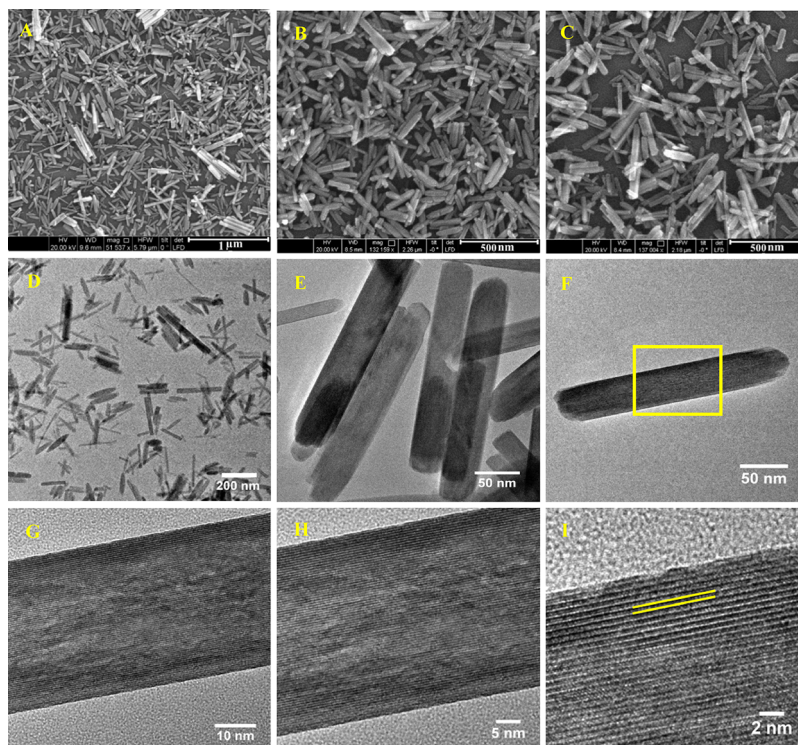
Figure 1. (A−C) FESEM and (D, E) TEM micrographs of FeOOH NRs at different magnifications. (F) TEM micrograph of a single FeOOH nanorod. (G−I) HRTEM images of FeOOH NRs at diverse magnifications.
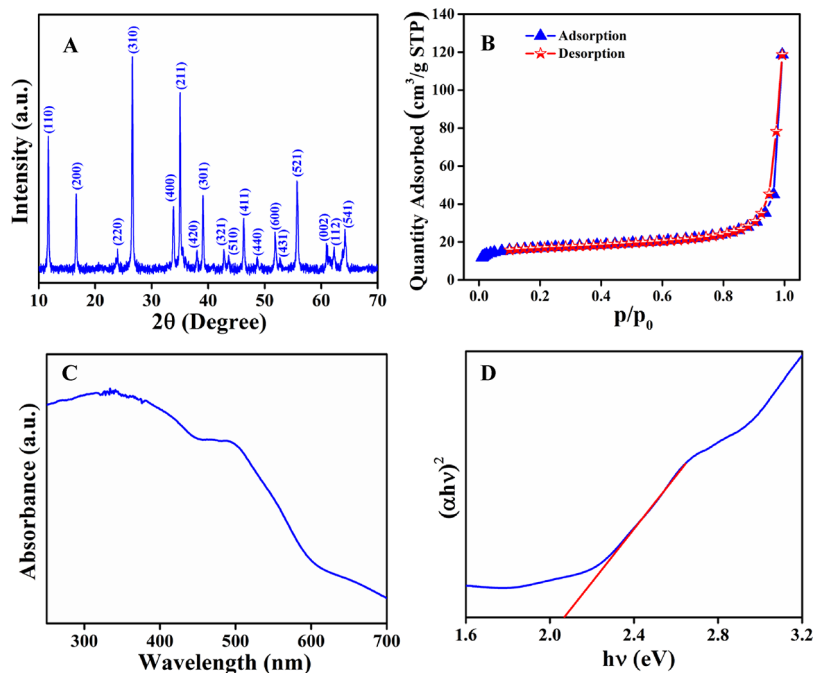

Figure 2. (A) XRD pattern and (B) nitrogen adsorption/desorption isotherms of β-FeOOH NRs. (C) UV−vis diffuse-reflectance spectra of the β-FeOOH NRs and (D) plot of $(\alpha h\nu)^2$ versus $h\nu$ for the β-FeOOH nanorods to calculate the band gap energy.

Figure 1G−I. The clear lattice fringes having a spacing of 0.53 nm corroborate to the (200) plane of β-FeOOH NR. We have then carried out energy-dispersive spectroscopy (EDS) analysis on FeOOH NRs, which corroborates to the presence of Fe and O in the nanorods, as presented in Figure S1.

The crystal structure of the as-prepared FeOOH NRs was investigated by X-ray diffraction (XRD) analysis (Figure 2A).

All the observed diffraction peaks could be well assigned to the pure tetragonal β-FeOOH phase (JCPDS no. 34-1266). No other characteristic peaks were observed for any kind of impurities. All the sharp peaks observed in the XRD patterns suggest well crystallization of the β-FeOOH NRs. The Fourier transform infrared (FTIR) spectrum of β-FeOOH NRs illustrates the presence of several bands at 3380, 1630, and
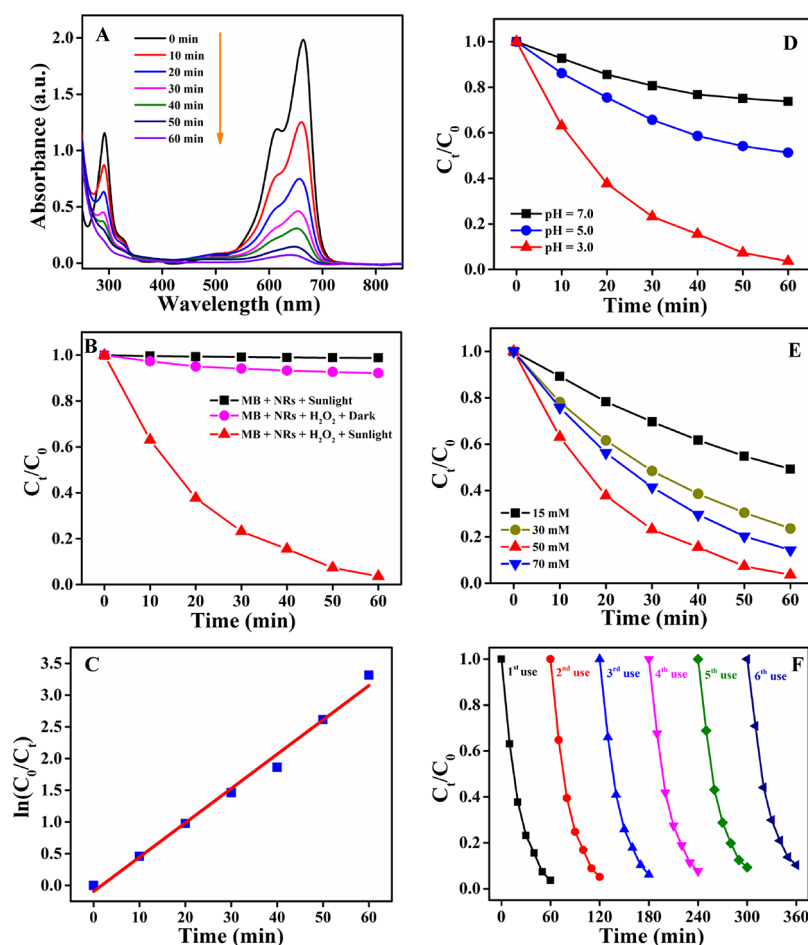
Figure 3. (A) Time-dependent UV−vis absorption spectra of the aqueous solution of MB during photodegradation using β-FeOOH NRs as catalysts in the presence of H_2O_2 under irradiation of sunlight. (B) Degradation efficiency toward MB in different reaction conditions. (C) Rate of degradation of MB using β-FeOOH NRs. (D) Photocatalytic activity of β-FeOOH NRs at different solution pH. (E) Effect of concentration of H_2O_2 on the photocatalytic activity of β-FeOOH NRs toward MB. (F) Multi-cycle degradation efficacy of β-FeOOH NRs during the degradation of MB under irradiation of sunlight.

1390 cm^{-1}, which can be attributed to the O−H stretching vibrations of absorbed water molecules or structural OH groups of NRs (Figure S2).[38] Additionally, two more peaks observed at 688 and 846 cm^{-1} are due to Fe−O vibrational modes of β-FeOOH.[39] N_2 adsorption/desorption analysis of the NRs was also carried out at 77 K to evaluate the specific surface area (Figure 2B). The specific surface area has been found to be 55 m^{2}g^{-1} for β-FeOOH NRs estimated using the Brunauer−Emmett−Teller (BET) method. The optical absorption property of β-FeOOH NRs was further established by performing their UV−vis DRS analysis, as shown in Figure 2C. The band gap energy (E_g) of β-FeOOH NRs has been estimated according to the following formula:[40,41] $\alpha h\nu = A(h\nu - E_g)^{1/2}$, where α, h, ν, E_g, and A are the absorption coefficient, Planck's constant, light frequency, the band gap energy, and a constant, respectively. We have then calculated the E_g for β-FeOOH NRs, which has been found to be 2.06 eV (Figure 2D). This is in accordance with the reported result.[42]

The photocatalytic efficacy of β-FeOOH NRs toward the degradation of organic dyes was studied under solar light irradiation. For this purpose, we have taken methylene blue (MB) and rhodamine B (RhB) as model pollutants. After reaching the adsorption/desorption equilibrium, dye solution was irradiated under sunlight in the presence of H_2O_2 and the UV-visible absorption spectra of the dye solution were

recorded as a function of irradiated time during the photodegradation process. The time-dependent degradation of MB by β-FeOOH NRs at pH 3 is presented in Figure 3A. During the degradation process, the color of MB solution progressively transformed from blue to pale blue and finally became colorless. Keeping the irradiation time unaltered, we also examined the photocatalytic efficacy of β-FeOOH NRs in different reaction conditions. We observed that there was almost no degradation of MB in the presence of only β-FeOOH NRs under solar light (Figure 3B), but the degradation efficiency of β-FeOOH NRs increased to approximately 100% within 60 min in the presence of H_2O_2 under sunlight. However, in the presence of both β-FeOOH NRs and H_2O_2 under dark conditions, the degradation of MB was estimated to be almost 8%. Similarly, upon exposure of sunlight on RhB solution, the bright red aqueous solution of RhB gradually faded away and finally turned out to be colorless in about 100 min (Figure S3). In photo-Fenton reaction, the synergistic effect of sunlight and H_2O_2 facilitates the formation of an enormous amount of hydroxyl radicals ($\cdot$OH) that boost the dye degradation process. To estimate the optimum catalyst dose, the degradation reaction was performed by changing the dosages of the catalyst. After carrying out the degradation reaction with different amounts of β-FeOOH NRs, the catalyst

dose was optimized and found to be 0.25 g L^{-1} for this photo-Fenton reaction (Figure S4).

Langmuir−Hinshelwood (LH) kinetics is the most frequently used kinetic expression to describe the kinetics of the heterogeneous catalytic processes.[43,44] The expression is given by

$$r = -dC/dt = k_r K_e C/(1 + K_e C) \tag{1}$$

where r represents the rate of reaction that changes with time. C is the concentration (mg L^{-1}) of the dye solution, which is being degraded, and k_r and K_e are the reaction rate constant (mg L^{-1} min^{-1}) and equilibrium constant (L mg^{-1}) for the adsorption of the dye molecules on the catalyst surface, respectively. The term $k_r K_e$ is considered as k (min^{-1}). Thus, eq 1 can be written as

$$r = -dC/dt = kC/(1 + K_e C) \tag{2}$$

When the chemical concentration C is a millimolar solution (for small C, $K_e C < 1$), eq 2 can be simplified to an apparent first-order equation

$$\text{Then,} \; -dC/dt = kC \; \text{or} \; -dC/C = k dt \tag{3}$$

Equation 3 can be integrated between the limits $C = C_0$ at $t = 0$ and $C = C_t$ at $t = t$. The integrated expression is given by $\ln(C_0/C_t) = kt$. Thus, the kinetics of photo-Fenton reaction using β-FeOOH NRs was further illustrated under solar light irradiation based on the above pseudo-first-order kinetic model: $\ln(C_0/C_t) = kt$,[45] where C_0 was the initial concentration of the dye, C_t was the concentration of the dye at the degradation time t, and k was the reaction rate constant. It was observed that the degradation of the dyes followed the pseudo-first-order kinetic model (Figure 3C), and the corresponding rate constants of the degradation of each dye were evaluated. The degradation time, percentage of degradation, and the first-order rate constants for each dye have been shown in Table 1.

Table 1. Summary of Degradation Time and Percentage of Degradation of Two Different Dyes Using β-FeOOH NRs under Irradiation of Sunlight with the Corresponding Rate Constant Evaluated Using the Pseudo-First-Order Kinetic Model

catalyst	name of dye	degradation time (min)	% of degradation	first-order rate constant (k, min^{-1})
β-FeOOH NRs	MB	60	97	0.05409
	RhB	100	96	0.02956

Generally, in photo-Fenton reaction, solution pH and concentration of H_2O_2 impart very significant roles. Keeping this idea in mind, the photocatalytic activity of β-FeOOH NRs was studied against varied pH of the dye solution (Figure 3D). It was found that the photocatalytic activity decreased with the increase in pH value. This is probably owing to the formation of a small amount of ·OH radicals at high solution pH in the course of the photo-Fenton process.[46] Moreover, the surface of the catalyst would gradually be deprotonated with increasing solution pH, which in turn lowered the adsorption of MB over NR surfaces.[47] Likewise, the photocatalytic activity of β-FeOOH NRs was evaluated as a function of H_2O_2 concentration, resulting in an increase in degradation rate with an increasing H_2O_2 concentration of up to 50 mM, as shown in Figure 3E. Interestingly, the rate of degradation was significantly decreased with a further increase in concentration

of H_2O_2 to 70 mM. This is possibly attributed to the scavenging effect of the hydroxyl radicals.[48,49] In the presence of excessive H_2O_2, ·OH radicals produce hydroperoxyl (·OOH) radicals, which do not participate in the degradation reaction owing to their much lower oxidation capacity.[50]

$$\cdot OH + H_2O_2 \rightarrow H_2O + \cdot OOH$$

$$\cdot OH + \cdot OOH \rightarrow H_2O + O_2$$
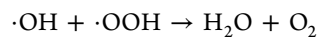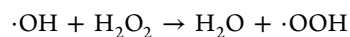
Basically, these auto-generated ·OOH radicals were responsible in lowering the degradation efficacy of a catalyst as they possessed much lesser oxidation potentials than the ·OH radical.[51] Additionally, excessive H_2O_2 may adsorb over the surface of the catalyst and thus inhibits the adsorption of MB, resulting in a decrease in degradation efficacy of the catalyst. Hence, it is necessary to find out the optimal concentration of H_2O_2 to enhance the degradation, beyond which it lowers the degradation efficacy of a catalyst. The threshold concentration of H_2O_2 for this particular degradation reaction was estimated to be 50 mM under mentioned reaction conditions.

To demonstrate the recyclability of β-FeOOH NRs, they have been used repetitively for dye degradation reaction (Figure 3F). After every use, the photocatalyst was easily recovered via centrifugation from the reaction solution and further employed for the next cycle. A reasonably good degradation efficacy of β-FeOOH NRs was noticed even after several usages, further demonstrating the exceptional advantage of utilization of β-FeOOH NRs as the photocatalyst from the effective separation and recycling point of view. We have also estimated the turn-over number (TON) and turn-over frequency (TOF) of the catalyst, which demonstrate the efficacy of a catalyst (please check the Supporting Information section). For this degradation reaction, the TON and TOF values were calculated to be 1.198×10^{20} molecules per gram and 0.332×10^{17} molecules per gram per second, respectively.

After the end of the photocatalytic reactions, we have performed the FESEM and TEM analysis of the catalyst to check their morphology change if it occurs. However, all the micrographs indicate their unaltered morphology even after reuse (Figure S5). Apart from these analyses, we have also carried out XRD analysis to specify whether there is any structural change of the NRs. Interestingly, the XRD pattern of the NRs after photocatalysis (Figure S6) is analogous to the fresh catalysts, with no alternation of their crystal structure, which again demonstrates their excellent durability and stability. Finally, the catalytic efficacy of β-FeOOH NRs was compared in associated with the reported oxide-based photocatalysts obtained by different synthesis routes for dye degradation (presented in Table S1), substantiating a much higher catalytic performance of our β-FeOOH NRs synthesized via a light-assisted hydrolysis route.

The dye degradation reaction using β-FeOOH NRs under solar light irradiation proceeds via photo-generated reactive oxygen species (ROS), mainly hydroxyl (·OH) radicals, superoxide (·O_2^-) radicals, and holes (h^+).[52,53] Basically, due to the irradiation of solar light onto the semiconductor photocatalysts, electrons in the valence band (VB) get excited and move to the conduction band (CB), resulting in the formation holes in the VB. These photo-generated holes (h^+) and electrons (e^-) function as primary reactive species and take part directly or indirectly in the degradation process through redox reactions.[54] The proposed dye degradation

mechanism using β-FeOOH NRs under solar light irradiation via photo-generated reactive oxygen species is illustrated in Figure 4. The photo-generated h$^+$ directly acts as an oxidant
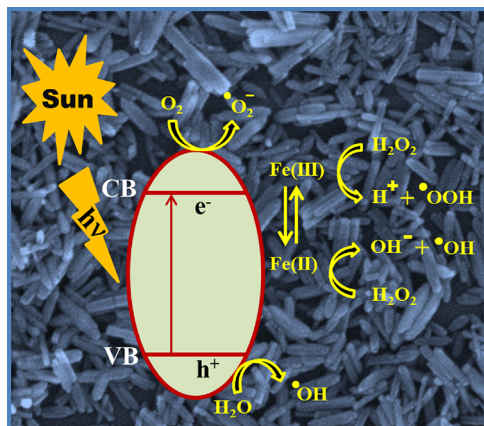

Figure 4. Proposed dye degradation mechanism using β-FeOOH NRs under solar light irradiation via photo-generated reactive oxygen species.

during the degradation of the pollutant, whereas electrons (e$^-$) react with O_2 present in the aqueous solution producing $\cdot O_2^-$ radicals. Usually in the photo-Fenton reaction, $\cdot$OH radicals are produced due to the transfer of electrons between Fe(II)/Fe(III) and H_2O_2.[55]

$$Fe(III) + H_2O_2 \rightarrow Fe(II) + H^+ + \cdot OOH$$

$$Fe(II) + H_2O_2 \rightarrow Fe(III) + OH^- + \cdot OH$$
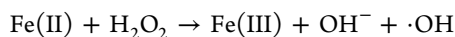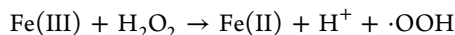
These photo-generated $\cdot$OH radicals take part in dye degradation and are mainly responsible in enhancing the degradation process. To confirm the generation of $\cdot$OH radicals, we performed the degradation process in the presence of *tert*-butanol (*t*-BuOH), which acts as the $\cdot$OH radical scavenger.[18,56,57] In the presence of *t*-BuOH, the degradation rate of MB was drastically reduced (Figure S7). Thus, insights into the dye degradation using iron oxide-based materials further point to the fundamental significance in understanding the photocatalysis and at the same time extending the broad applicability of such naturally occurring semiconducting nanomaterials.

CONCLUSIONS

In summary, we have described a facile route to synthesize iron oxide nanorods without employing any templating agent via a light-driven hydrolysis route. After characterization of synthesized nanorods by different physical techniques, the photocatalytic activity of as-synthesized β-FeOOH nanorods was explored as a photo-Fenton catalyst under sunlight. Methylene blue (MB) and rhodamine B (RhB) were chosen as model refractory pollutants to demonstrate the photocatalytic performance of β-FeOOH nanorods. The effect of pH of the solution together with concentration of H_2O_2 on their photocatalytic activity has also been demonstrated. The overall dye degradation under solar light irradiation using β-FeOOH NRs proceeds via photo-generated reactive oxygen species. Our approach thus points to an excellent photo-catalytic activity of β-FeOOH nanorods during the photo-Fenton reaction. This work offers an environmentally friendly and

cost-effective way to develop highly active photocatalytic nanomaterials to combat with environmental pollutants.

ASSOCIATED CONTENT

ⓢ Supporting Information

The Supporting Information is available free of charge at https://pubs.acs.org/doi/10.1021/acsomega.1c03617.

Characterization techniques, EDX spectrum and FTIR spectra of β-FeOOH nanorods, time-dependent UV-visible absorption spectra of RhB and rate of degradation of RhB using β-FeOOH NRs, the effect of catalyst dose, estimation of TON and TOF, the effect of *t*-BuOH on the degradation efficiency of β-FeOOH NRs, XRD patterns, FESEM, and TEM images of β-FeOOH NRs after photocatalysis, and comparison of photocatalytic efficiency with the reported catalysts (PDF)

AUTHOR INFORMATION

Corresponding Authors

Samir Kumar Pal — *Department of Chemical, Biological & Macro-Molecular Sciences, S. N. Bose National Centre for Basic Sciences, Kolkata 700 106, India; Technical Research Centre, S. N. Bose National Centre for Basic Sciences, Kolkata 700 106, India;* ⓞ orcid.org/0000-0001-6943-5828; Email: skpal@bose.res.in

Subhra Jana — *Department of Chemical, Biological & Macro-Molecular Sciences, S. N. Bose National Centre for Basic Sciences, Kolkata 700 106, India; Technical Research Centre, S. N. Bose National Centre for Basic Sciences, Kolkata 700 106, India;* ⓞ orcid.org/0000-0002-7105-7106; Phone: +9133 2335 5706; Email: subhra.jana@bose.res.in

Author

Arnab Samanta — *Department of Chemical, Biological & Macro-Molecular Sciences, S. N. Bose National Centre for Basic Sciences, Kolkata 700 106, India*

Complete contact information is available at:
https://pubs.acs.org/10.1021/acsomega.1c03617

Notes

The authors declare no competing financial interest.

ACKNOWLEDGMENTS

REFERENCES

(1) Hoffmann, M. R.; Martin, S. T.; Choi, W.; Bahnemann, D. W. Environmental Applications of Semiconductor Photocatalysis. *Chem. Rev.* **1995**, *95*, 69−96.

(2) Schwarzenbach, R. P.; Egli, T.; Hofstetter, T. B.; Von Gunten, U.; Wehrli, B. Global Water Pollution and Human Health. *Annu. Rev. Environ. Resour.* **2010**, *35*, 109−136.

(3) Sires, I.; Brillas, E. Remediation of Water Pollution Caused by Pharmaceutical Residues Based on Electrochemical Separation and Degradation Technologies: A Review. *Environ. Int.* **2012**, *40*, 212−229.

(4) Qian, J.; Gao, X.; Pan, B. Nanoconfinement-Mediated Water Treatment: From Fundamental to Application. *Environ. Sci. Technol.* **2020**, *54*, 8509−8526.

(5) Dong, S.; Feng, J.; Fan, M.; Pi, Y.; Hu, L.; Han, X.; Liu, M.; Sun, J.; Sun, J. Recent Developments in Heterogeneous Photocatalytic Water Treatment using Visible Light-Responsive Photocatalysts: A Review. *RSC Adv.* **2015**, *5*, 14610−14630.

(6) Mills, A.; Davies, R. H.; Worsley, D. Water Purification by Semiconductor Photocatalysis. *Chem. Soc. Rev.* **1993**, *22*, 417−425.

(7) Grau, P. Textile Industry Wastewaters Treatment. *Water Sci. Technol.* **1991**, *24*, 97−103.

(8) Sanjini, N. S.; Velmathi, S. Photocatalytic Degradation of Rhodamine B by Mesoporous Ti-KIT-6 under UV Light and Solar Light Irradiation. *J. Porous Mater.* **2015**, *22*, 1549−1558.

(9) Weber, E. J.; Adams, R. L. Chemical- and Sediment-Mediated Reduction of the Azo Dye Disperse Blue 79. *Environ. Sci. Technol.* **1995**, *29*, 1163−1170.

(10) Steplin, S. S. P.; Radhika, N.; Borang, O.; Lydia, I. S.; Merlin, J. P. Visible Light Driven Photodegradation of Rhodamine B using Cysteine Capped ZnO/GO Nanocomposite as Photocatalyst. *J. Mater. Sci.: Mater. Electron.* **2017**, *28*, 6722−6730.

(11) Guo, J.; Yuan, S.; Jiang, W.; Yue, H.; Cui, Z.; Liang, B. Adsorption and Photocatalytic Degradation Behaviors of Rhodamine Dyes on Surface-Fluorinated TiO_2 under Visible Irradiation. *RSC Adv.* **2016**, *6*, 4090−4100.

(12) Zhao, R.; Wang, Y.; Li, X.; Sun, B.; Wang, C. Synthesis of β-Cyclodextrin-Based Electrospun Nanofiber Membranes for Highly Efficient Adsorption and Separation of Methylene Blue. *ACS Appl. Mater. Interfaces* **2015**, *7*, 26649−26657.

(13) Luan, J.; Hou, P. X.; Liu, C.; Shi, C.; Li, G. X.; Cheng, H. M. Efficient Adsorption of Organic Dyes on a Flexible Single-Wall Carbon Nanotube Film. *J. Mater. Chem. A* **2016**, *4*, 1191−1194.

(14) Song, S.; Wang, Y.; Shen, H.; Zhang, J.; Mo, H.; Xie, J.; Zhou, N.; Shen, J. Ultrasmall Graphene Oxide Modified with Fe_3O_4 Nanoparticles as a Fenton-Like Agent for Methylene Blue Degradation. *ACS Appl. Nano Mater.* **2019**, *2*, 7074−7084.

(15) Ismael, M.; Wu, Y. A Facile Synthesis Method for Fabrication of $LaFeO_3/gC_3N_4$ Nanocomposite as Efficient Visible-Light-Driven Photocatalyst for Photodegradation of RhB and 4-CP. *New J. Chem.* **2019**, *43*, 13783−13793.

(16) Kimling, M. C.; Chen, D.; Caruso, R. A. Temperature-Induced Modulation of Mesopore Size in Hierarchically Porous Amorphous TiO_2/ZrO_2 Beads for Improved Dye Adsorption Capacity. *J. Mater. Chem. A* **2015**, *3*, 3768−3776.

(17) Huang, L.; He, M.; Chen, B.; Cheng, Q.; Hu, B. Facile Green Synthesis of Magnetic Porous Organic Polymers for Rapid Removal and Separation of Methylene Blue. *ACS Sustainable Chem. Eng.* **2017**, *5*, 4050−4055.

(18) Das, S.; Samanta, A.; Jana, S. Light-Assisted Synthesis of Hierarchical Flower-Like MnO_2 Nanocomposites with Solar Light Induced Enhanced Photocatalytic Activity. *ACS Sustainable Chem. Eng.* **2017**, *5*, 9086−9094.

(19) Yu, C.; Li, G.; Kumar, S.; Yang, K.; Jin, R. Phase Transformation Synthesis of Novel Ag_2O/Ag_2CO_3 Heterostructures with High Visible Light Efficiency in Photocatalytic Degradation of Pollutants. *Adv. Mater.* **2014**, *26*, 892−898.

(20) Yang, Y.; Li, J.; Wang, H.; Song, X.; Wang, T.; He, B.; Liang, X.; Ngo, H. H. An Electrocatalytic Membrane Reactor with Self-Cleaning Function for Industrial Wastewater Treatment. *Angew. Chem., Int. Ed.* **2011**, *50*, 2148−2150.

(21) Tusar, N. N.; Maučec, D.; Rangus, M.; Arčon, I.; Mazaj, M.; Cotman, M.; Pintar, A.; Kaučič, V. Manganese Functionalized Silicate Nanoparticles as a Fenton-type Catalyst for Water Purification by Advanced Oxidation Processes (AOP). *Adv. Funct. Mater.* **2012**, *22*, 820−826.

(22) Vu, T. A.; Le, G. H.; Dao, C. D.; Dang, L. Q.; Nguyen, K. T.; Dang, P. T.; Tran, H. T.; Duong, Q. T.; Nguyen, T. V.; Lee, G. D. Isomorphous Substitution of Cr by Fe in MIL-101 Framework and Its Application as a Novel Heterogeneous Photo-Fenton Catalyst for Reactive Dye Degradation. *RSC Adv.* **2014**, *4*, 41185−41194.

(23) Zhang, Y.; Zhang, N.; Wang, T.; Huang, H.; Chen, Y.; Li, Z.; Zou, Z. Heterogeneous Degradation of Organic Contaminants in the

Photo-Fenton Reaction Employing Pure Cubic β-Fe_2O_3. *Appl. Catal. B* **2019**, *245*, 410−419.

(24) Yang, Y.; Pignatello, J. J.; Ma, J.; Mitch, W. A. Comparison of Halide Impacts on the Efficiency of Contaminant Degradation by Sulfate and Hydroxyl Radical-Based Advanced Oxidation Processes (AOPs). *Environ. Sci. Technol.* **2014**, *48*, 2344−2351.

(25) Zhang, C.; Ou, Y.; Lei, W. X.; Wan, L. S.; Ji, J.; Xu, Z. K. $CuSO_4/H_2O_2$-Induced Rapid Deposition of Polydopamine Coatings with High Uniformity and Enhanced Stability. *Angew. Chem. Int. Ed.* **2016**, *55*, 3054−3057.

(26) Liu, Y.; Jin, W.; Zhao, Y.; Zhang, G.; Zhang, W. Enhanced Catalytic Degradation of Methylene Blue by α-Fe_2O_3/Graphene Oxide via Heterogeneous Photo-Fenton Reactions. *Appl. Catal., B* **2017**, *206*, 642−652.

(27) Qian, X.; Ren, M.; Zhu, Y.; Yue, D.; Han, Y.; Jia, J.; Zhao, Y. Visible Light Assisted Heterogeneous Fenton-Like Degradation of Organic Pollutant via α-FeOOH/Mesoporous Carbon Composites. *Environ. Sci. Technol.* **2017**, *51*, 3993−4000.

(28) Tian, H.; Peng, J.; Du, Q.; Hui, X.; He, H. One-pot sustainable synthesis of Magnetic MIL-100 (Fe) with Novel Fe_3O_4 Morphology and Its Application in Heterogeneous Degradation. *Dalton Trans.* **2018**, *47*, 3417−3424.

(29) Wang, X.; Wang, J.; Cui, Z.; Wang, S.; Cao, M. Facet Effect of α-Fe_2O_3 Crystals on Photocatalytic Performance in the Photo-Fenton Reaction. *RSC Adv.* **2014**, *4*, 34387−34394.

(30) Chen, H.; Zhang, Z.; Yang, Z.; Yang, Q.; Li, B.; Bai, Z. Heterogeneous Fenton-like Catalytic Degradation of 2, 4-Dichlorophenoxyacetic Acid in Water with FeS. *Chem. Eng. J.* **2015**, *273*, 481−489.

(31) Huang, X.; Niu, Y.; Hu, W. Fe/Fe_3C Nanoparticles Loaded on Fe/N-Doped Graphene as an Efficient Heterogeneous Fenton Catalyst for Degradation of Organic Pollutants. *Colloids Surf., A* **2017**, *518*, 145−150.

(32) Shi, W.; Du, D.; Shen, B.; Cui, C.; Lu, L.; Wang, L.; Zhang, J. Synthesis of Yolk-Shell Structured Fe_3O_4@void@CdS Nanoparticles: A General and Effective Structure Design for Photo-Fenton Reaction. *ACS Appl. Mater. Interfaces* **2016**, *8*, 20831−20838.

(33) Samanta, A.; Das, S.; Jana, S. Doping of Ni in α-Fe 2 O 3 Nanoclews to Boost Oxygen Evolution Electrocatalysis. *ACS Sustainable Chem. Eng.* **2019**, *7*, 12117−12124.

(34) Samanta, A.; Jana, S. Ni-, Co-, and Mn-Doped Fe_2O_3 Nano-Parallelepipeds for Oxygen Evolution. *ACS Appl. Nano Mater.* **2021**, *4*, 5131−5140.

(35) He, L.; Tan, C.; Sheng, C.; Chen, Y.; Yu, F.; Chen, Y. A β-FeOOH/MXene Sandwich for High-Performance Anodes in Lithium-Ion Batteries. *Dalton Trans.* **2020**, *49*, 9268−9273.

(36) Wang, C.; Yang, X.; Zheng, M.; Xu, Y. Synthesis of β-FeOOH Nanorods Adhered to Pine-Biomass Carbon as A Low-Cost Anode Material for Li-Ion Batteries. *J. Alloys Compd.* **2019**, *794*, 569−575.

(37) Samanta, A.; Das, S.; Jana, S. Exploring β-FeOOH Nanorods as an Efficient Adsorbent for Arsenic and Organic Dyes. *ChemistrySelect* **2018**, *3*, 2467−2473.

(38) Wei, C.; Nan, Z. Effects of Experimental Conditions on One-Dimensional Single-Crystal Nanostructure of β-FeOOH. *Mater. Chem. Phys.* **2011**, *127*, 220−226.

(39) Mao, Y.; Jiang, W.; Xuan, S.; Fang, Q.; Leung, K. C. F.; Ong, B. S.; Wang, S.; Gong, X. Rod-Like β-FeOOH@Poly(Dopamine)-Au-Poly(Dopamine) Nanocatalysts with Improved Recyclable Activities. *Dalton Trans.* **2015**, *44*, 9538−9544.

(40) Jana, S.; Pande, S.; Sinha, A. K.; Sarkar, S.; Pradhan, M.; Basu, M.; Saha, S.; Pal, T. A Green Chemistry Approach for the Synthesis of Flower-Like Ag-Doped MnO_2 Nanostructures Probed by Surface-Enhanced Raman Spectroscopy. *J. Phys. Chem. C* **2009**, *113*, 1386−1392.

(41) Sultana, S.; Mansingh, S.; Parida, K. M. Rational Design of Light Induced Self Healed Fe Based Oxygen Vacancy Rich CeO_2 (CeO_2NS-$FeOOH/Fe_2O_3$) Nanostructure Materials for Photocatalytic Water Oxidation and Cr(VI) Reduction. *J. Mater. Chem. A* **2018**, *6*, 11377−11389.

(42) Xu, Z.; Yu, Y.; Fang, D.; Xu, J.; Liang, J.; Zhou, L. Microwave-Ultrasound Assisted Synthesis of β-FeOOH and Its Catalytic Property in a Photo-Fenton-Like Process. *Ultrason. Sonochem.* **2015**, *27*, 287−295.

(43) Mahamallik, P.; Pal, A. Photo-Fenton Process in a Co (II)-Adsorbed Micellar Soft-Template on an Alumina Support for Rapid Methylene Blue Degradation. *RSC Adv.* **2016**, *6*, 100876−100890.

(44) Konstantinou, I. K.; Albanis, T. A. Photocatalytic Transformation of Pesticides in Aqueous Titanium Dioxide Suspensions using Artificial and Solar Light: Intermediates and Degradation Pathways. *Appl. Catal., B* **2003**, *42*, 319−335.

(45) Das, S.; Jana, S. A Tubular Nanoreactor Directing the Formation of In Situ Iron Oxide Nanorods with Superior Photocatalytic Activity. *Environ. Sci.: Nano* **2017**, *4*, 596−603.

(46) Zhang, C.; Yang, H. C.; Wan, L. S.; Liang, H. Q.; Li, H.; Xu, Z. K. Polydopamine-Coated Porous Substrates as a Platform for Mineralized β-FeOOH Nanorods with Photocatalysis under Sunlight. *ACS Appl. Mater. Interfaces* **2015**, *7*, 11567−11574.

(47) Xu, Z.; Liang, J.; Zhou, L. Photo-Fenton-Like Degradation of Azo Dye Methyl Orange using Synthetic Ammonium and Hydronium Jarosite. *J. Alloys Compd.* **2013**, *546*, 112−118.

(48) Feng, J.; Hu, X.; Yue, P.; Zhu, H.; Lu, G. Degradation of Azo-Dye Orange II by a Photoassisted Fenton Reaction Using a Novel Composite of Iron Oxide and SilicateNanoparticles as a Catalyst. *Ind. Eng. Chem. Res.* **2003**, *42*, 2058−2066.

(49) Zhao, Y.; Hu, J.; Jin, W. Transformation of Oxidation Products and Reduction of Estrogenic Activity of 17β-Estradiol by a Heterogeneous Photo-Fenton Reaction. *Environ. Sci. Technol.* **2008**, *42*, 5277−5284.

(50) Ahmed, Y.; Yaakob, Z.; Akhtara, P. Degradation and Mineralization of Methylene Blue Using a Heterogeneous Photo-Fenton Catalyst under Visible and Solar Light Irradiation. *Catal. Sci. Technol.* **2016**, *6*, 1222−1232.

(51) Cheng, M.; Liu, Y.; Huang, D.; Lai, C.; Zeng, G.; Huang, J.; Liu, Z.; Zhang, C.; Zhou, C.; Qin, L.; Xiong, W.; Yi, H.; Yang, Y. Prussian Blue Analogue Derived Magnetic Cu-Fe Oxide as a Recyclable Photo-Fenton Catalyst for the Efficient Removal of Sulfamethazine at Near Neutral pH Values. *Chem. Eng. J.* **2019**, *362*, 865−876.

(52) Nosaka, Y.; Nosaka, A. Y. Generation and Detection of Reactive Oxygen Species in Photocatalysis. *Chem. Rev.* **2017**, *117*, 11302−11336.

(53) Chen, C.; Ma, W.; Zhao, J. Semiconductor-Mediated Photodegradation of Pollutants under Visible-Light Irradiation. *Chem. Soc. Rev.* **2010**, *39*, 4206−4219.

(54) Banerjee, S.; Pillai, S. C.; Falaras, P.; O'shea, K. E.; Byrne, J. A.; Dionysiou, D. D. New Insights into the Mechanism of Visible Light Photocatalysis. *J. Phys. Chem. Lett.* **2014**, *5*, 2543−2554.

(55) Hartmann, M.; Kullmann, S.; Keller, H. Wastewater Treatment with Heterogeneous Fenton-Type Catalysts Based on Porous Materials. *J. Mater. Chem.* **2010**, *20*, 9002−9017.

(56) Guo, T.; Jiang, L.; Wang, K.; Li, Y.; Huang, H.; Wu, X.; Zhang, G. Efficient Persulfate Activation by Hematite Nanocrystals for Degradation of Organic Pollutants under Visible Light Irradiation: Facet-Dependent Catalytic Performance and Degradation Mechanism. *Appl. Catal., B* **2021**, *286*, 119883.

(57) Huang, H.; Guo, T.; Wang, K.; Li, Y.; Zhang, G. Efficient Activation of Persulfate by a Magnetic Recyclable Rape Straw Biochar Catalyst for the Degradation of Tetracycline Hydrochloride in Water. *Sci. Total Environ.* **2021**, *758*, 143957.